Label-Free Quantitative Detection of Protein Using Macroporous Silicon Photonic Bandgap Biosensors

ARTICLE *in* ANALYTICAL CHEMISTRY · MARCH 2007

Impact Factor: 5.64 · DOI: 10.1021/ac0608366 · Source: PubMed

4 AUTHORS, INCLUDING:

Lisa A Delouise
University of Rochester
78 PUBLICATIONS **1,893** CITATIONS

SEE PROFILE

Anal. Chem. **2007,** *79,* 1502−1506

Label-Free Quantitative Detection of Protein Using Macroporous Silicon Photonic Bandgap Biosensors

Huimin Ouyang,*,†,‡ Lisa A. DeLouise,†,§ Benjamin L. Miller,†,§ and Philippe M. Fauchet†,‡

Center for Future Health, University of Rochester, Rochester, New York 14642, Department of Electrical and Computer Engineering, University of Rochester, Rochester, New York 14627, and Department of Dermatology, University of Rochester, New York 14642

A label-free biosensor was demonstrated using macroporous silicon (pore size >100 nm) one-dimensional photonic band gap structures that are very sensitive to refractive index changes. In this study, we employed Tir−IBD (translocated Intimin receptor−Intimin binding domain) and Intimin−ECD (extracellular domain of Intimin) as the probe and target, respectively. These two recombinant proteins comprise the extracellular domains of two key proteins responsible for the pathogenicity of enteropathogenic *Escherichia coli* (EPEC). The optical response of the sensor was characterized so that the capture of Intimin−ECD could be quantitatively determined. Our result shows that the concentration sensitivity limit of the sensor is currently 4 μM of Intimin−ECD. This corresponds to a detection limit of approximately 130 fmol of Intimin−ECD. We have also investigated the dependence of the sensor performance on the Tir−IBD probe molecule concentration and the effect of immobilization on the Tir−IBD/Intimin−ECD equilibrium dissociation constant. A calibration curve generated from purified Intimin−ECD solutions was used to quantify the concentration of Intimin−ECD in an *E. coli* BL21 bacterial cell lysate, and results were validated using gel electrophoresis. This work demonstrates for the first time that a macroporous silicon microcavity sensor can be used to selectively and quantitatively detect a specific target protein with micromolar dissociation constant (K_d) in a milieu of bacterial proteins with minimal sample preparation.

Over the past 2 decades, the development of label-free optical biosensors has been pursued with great interest by many researchers. Methods including surface plasmon resonance (SPR)[1] and interferometry[2,3] have been employed in label-free affinity biosensors to measure the change of refractive index at the surface of the sensor upon binding of the target molecules to the bioreceptors. Recently, there has been interest in using photonic band gap (PBG) structures for sensing applications.[4−6] The PBG structures are highly sensitive to changes in the refractive index of the environment because these changes occur where the electric field is maximum.[7] This makes PBG structures an ideal candidate for ultrasmall and efficient "lab-on-a-chip" devices.

Porous silicon (PSi)-based PBG structures have been investigated by many groups as an optical label-free sensing platform for chemical and biological detection.[4,8−10] The advantages of using PSi include ease of fabrication and compatibility with silicon microelectronics technology. The large internal surface area of PSi can be chemically modified for the capture and selective detection of different types of molecules, such as DNA,[2,5,11] proteins,[12−14] gram-negative bacteria,[9] and enzymes.[15] PSi membranes can also be released from the silicon substrate and used for in vivo applications as a "smart bandage"[16] and "smart dust".[17] The nanomorphology of the porous silicon layers is critical for biosensing applications. The pore size not only determines the size of the molecules that can infiltrate the pores but it also impacts the sensor sensitivity. The ultimate sensitivity performance of porous silicon sensors with different pore sizes was recently quantified using aminopropyltriethoxysilane (APTES) and glut-

* To whom correspondence should be addressed. Phone: 585-275-1252. Fax: 585-275-2073. E-mail: ouyang@ece.rochester.edu.

† Center for Future Health.

‡ Department of Electrical and Computer Engineering.

§ Department of Dermatology.

(1) Liedberg, B.; Nylander, C.; Lundstrom, I. *Sens. Actuators* **1983**, *4*, 299−304.

(2) Lin, V. S.; Motesharei, K.; Dancil, K. S.; Sailor, M. J.; Ghadiri, M. R.; *Science* **1997**, *278*, 840−843.

(3) Lukosz, W. *Sens. Actuators, B* **1995**, *29*, 37−50.

(4) Cunin, F.; Schmedake, T. A.; Link, J. R.; Li, Y. Y.; Koh, J.; Bhatia, S. N.; Sailor, M. J. *Nat. Mater.* **2002**, *1*, 39−41.

(5) Chan, S.; Li, Y.; Rothberg, L. J.; Miller, B. L.; Fauchet, P. M. *Mater. Sci. Eng., C* **2001**, *15*, 277−282.

(6) Chow, E.; Grot, A.; Mirkarimi, L. W.; Sigalas, M.; Girolami, G. *Opt. Lett.* **2004**, *29*, 1093−1095.

(7) Scheuer, J.; Green, W. M. G.; DeRose, G. A.; Yariv, A. *IEEE J. Sel. Top. Quantum Electron.* **2005**, *11*, 476−484.

(8) Mulloni, V.; Pavesi, L. *Appl. Phys. Lett.* **2000**, *76*, 2523−2525.

(9) Chan, S.; Horner, S. R.; Fauchet, P. M.; Miller, B. L. *J. Am. Chem. Soc.* **2001**, *123*, 11797−11798.

(10) Chan, S.; Fauchet, P. M.; Li, Y.; Rothberg, L. J.; Miller, B. L. *Phys. Status Solidi A* **2000**, *182*, 541−546.

(11) Archer, M.; Christophersen, M.; Fauchet, P. M. *Biomed. Microdevices* **2004**, *6*, 203−211.

(12) Ouyang, H.; Christophersen, M.; Viard, R.; Miller, B. L.; Fauchet, P. M. *Adv. Funct. Mater.* **2005**, *15*, 1851−1859.

(13) Dancil, K. P. S.; Greiner, D. P.; Sailor, M. J. *J. Am. Chem. Soc.* **1999**, *121*, 7925−7930.

(14) Zangooie, S.; Bjorklund, R.; Arwin, H. *Thin Solid Films* **1998**, *313*, 825−830.

(15) DeLouise, L. A.; Kou, P. M.; Miller, B. L. *Anal. Chem.* **2005**, *77*, 322−3230.

(16) DeLouise, L. A.; Fauchet, P. M.; Miller, B. L.; Pentland, A. A. *Adv. Mater.* **2005**, *17*, 2199−2203.

(17) Schemedake, T. A.; Cunin, F.; Link, J. R.; Sailor, M. J. *Adv. Mater.* **2002**, *14*, 1270−1272.

10.1021/ac0608366 CCC: $37.00
Published on Web 01/23/2007

araldehyde.[18] Although the sensitivity of the biosensor decreases as the pore size increases, large size pores (>100 nm) are useful for the detection of macromolecules (e.g., immunoglobin) that cannot infiltrate into devices with small pores (<30 nm). The PSi PBG structures with pore diameters in the 20−50 nm range are well suited for the detection of smaller molecules (<50 kDa). Recently, we have demonstrated the fabrication of a new type of macroporous silicon 1D PBG microcavity sensor which has pore diameters exceeding 100 nm.[12] The macropores allow easy infiltration and stacking of large size targets such as streptavidin (68 kDa) and biotinylated IgG (150 kDa).

To further explore the capability of macroporous 1D PBG sensors for protein detection, we investigated the design of a sensor for label-free detection of pathogenic *Escherichia coli* (*E. coli*). Our sensor was designed employing recombinant proteins corresponding to the extracellular domain of Intimin and Tir (translocated Intimin receptor), which are two proteins expressed by the enteropathogenic (EPEC) and the enterohemerogaic (EHEC) *E. coli* strains via the type III secretory pathway.[19] Both proteins are essential components of this organism's pathogenicity. The dissociation constant (K_d) of Tir−IBD (translocated Intimin receptor−Intimin binding domain) and Intimin−ECD (Intimin extracellular domain) is about 0.3 μM,[20] which is considerably weaker than in the biotin−streptavidin model system used in our previous work.[12] Hence, the Tir−IBD/Intimin−ECD system will enable us to determine the impact of the increased off-rate on detection sensitivity and the quantitative analytical performance of this device. Sensors were prepared by immobilizing the extracellular portion of Tir−IBD in the macroporous silicon microcavity as the probe molecule (the bioreceptor). The Tir−IBD-functionalized sensors were tested to determine the limit of Intimin−ECD protein detection in solution. We also investigated the utility of the sensor for quantitative analysis, the dependence of the sensor performance on the probe molecule concentration, and the ability of the sensor to selectively and quantitatively detect Intimin−ECD expression in the supernatant of an *E. coli* bacterial (Bl21) cell lysate relative to a control (JM109) cell lysate.

EXPERIMENTAL SECTION

Porous Silicon Microcavity Preparation. The fabrication of macroporous silicon microcavities has been described in detail elsewhere.[12] Macroporous silicon 1D PBG microcavities were electrochemically synthesized from n-type silicon wafers with 0.01 ohm-cm resistivity (from SEH Inc.) using an electrolyte solution containing 5.5% hydrofluoric acid (HF), 94% H_2O, and 0.5% surfactant (polyoxyalkylene alkyl ether from Wako Chemicals U.S.A. Inc.). The etching area of each sensor was approximately 150 mm^2. During the microcavity formation, the etching current density j alternated between 40 and 34 mA/cm^2 to form multilayer microcavities consisting of layers with distinct porosities. A very low porosity contrast was chosen (~80% vs ~70%) in order to keep the pores as large as possible throughout the entire structure. The microcavities consisted of two eight-period Bragg mirrors and a defect layer of a half-wavelength optical thickness. Cross-sectional and top view scanning electron micrographs (SEM) of a microcavity sensor are shown in Figure 1a−c . The average pore diameter was approximately 120 nm, and the total thickness of the sensor was ~5 μm. The optical reflectance spectra of the porous silicon microcavities were taken using an Ocean Optics HR 2000 spectrometer (550−950 nm) with a reflection probe R200-7 and an Ocean Optics LS-1 tungsten halogen light source. The illumination spot size was approximately 1 mm^2.

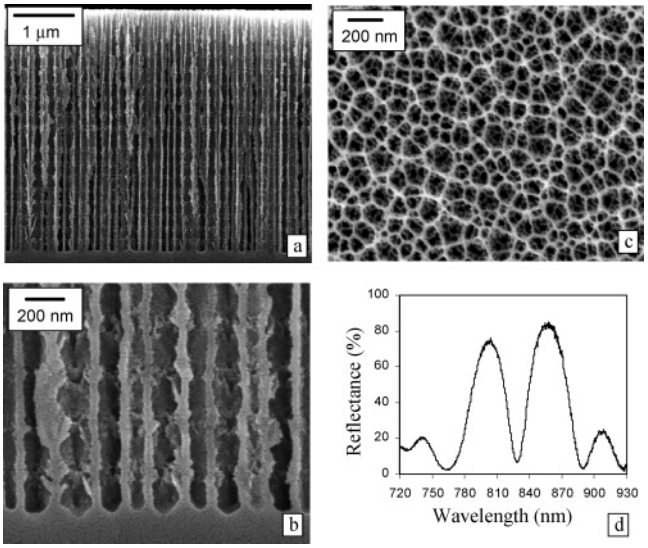

Figure 1. (a and b) Cross-sectional SEM images of a macroporous silicon microcavity with pore size approximately 120 nm. (c) Top view SEM image of a macroporous silicon microcavity. (d) Reflectance spectrum of a macroporous silicon microcavity, showing the reflectance dip near 830 nm.

After anodization, the microcavities were thermally oxidized at 900 °C for 3 min to form a silica-like internal surface. The spectrum blue shifted by approximately 100 nm after the oxidation, as part of the silicon was converted into SiO_2, which has a lower refractive index.

Protein Preparation. Details of the purification and quantification of the proteins has been described previously by Horner et al.[20] Independent overnight cultures in LB (Luria−Bertani) broth medium of the transformed *E. coli* BL21-expressing 6×His−Tir−IBD (~10 kDa) and 6×His−Intimin−ECD (32 kDa) were grown at 37 °C to OD 0.6 (measured at 595 nm) and induced with 1 mM IPTG overnight at room temperature. Tir−IBD and Intimin−ECD were purified using Amersham Biosciences-HiTrap chelating columns and dialyzed in HEPES buffer (20 mM HEPES, 150 mM NaCl, pH 7.5). The concentrations of the purified proteins were determined by OD at 280 nm using molar extinction coefficients ($\epsilon^{Tir} = 705$, $\epsilon^{intimin} = 36\,960$).

Sensor Functionalization. The probe molecule (Tir−IBD) was immobilized on the porous silicon matrix using standard aminopropyltriethoxysilane (APTES) and glutaraldehyde coupling chemistry. Each sensor was treated with 50 μL of 2% 3-aminopropyltriethoxysilane (Gelest Inc.) in 48% methanol and 50% H_2O for 20 min. The silane is rapidly hydrolyzed in water, which facilitates the condensation reaction to surface hydroxyl group on the PSi surface. The sensors were then rinsed with water and baked in an oven at 100 °C for 10 min. Following the silane treatment, 50 μL of 2.5% glutaraldehyde (Sigma) solution in 20 mM HEPES

(18) Ouyang, H.; Striemer, C. C.; Fauchet, P. M. *Appl. Phys. Lett.* **2006**, *88*, 163108.
(19) Zaharik, M. L.; Gruenheid, S.; Perrin, A. J.; Finlay, B. B. *Int. J. Med. Microbiol.* **2002**, *291*, 593−603.
(20) Horner, S. R.; Mace, C. R.; Rothberg, L. J.; Miller, B. L. *Biosens. Bioelectron.* **2006**, *21*, 1659−1663.

buffer (pH 7.3) was applied to each sensor for 30 min. Sensors were rinsed with HEPES buffer and dried in a stream of nitrogen. Next, a series of sensors were fabricated by applying 50 μL of Tir−IBD with concentrations ranging between 0 and 1 mM. Sensors were exposed to the Tir−IBD solution for 1 h. To prevent nonspecific attachment of Intimin−ECD to unreacted glutaraldehyde sites, each sensor was exposed to 50 μL of 1 M glycine methyl ester for 1 h (pH 5). After this treatment, each sensor was rinsed and soaked in HEPES buffer for 20 min and dried with nitrogen flow before exposure to the target solution.

Target Incubation, Protein Supernatant, and Controls. For target incubation, 50 μL of the Intimin−ECD solution (5−60 μM) was applied to the sensor for 1 h, and then rinsed/soaked with HEPES buffer for 1 ~ 2 h and dried with nitrogen flow before the optical measurement. This step was key to minimizing false positive signal from trapping of nonspecifically bound protein in the porous matrix. To determine the selectivity of the sensor to Intimin−ECD, independent overnight cultures of *E. coli* cells expressing Intimin−ECD and JM109 (stratagene) which does not express Intimin−ECD were grown up, centrifuged, lysed, and then resuspended in HEPES buffer (pH = 7.5). The supernatant solution was filtered through a 0.45 μm filter before exposure to the sensor. The presence or absence of Intimin−ECD in the protein supernatants from the Intimin−ECD-expressing *E. coli* cell line and JM109 was verified using SDS−PAGE gel electrophoresis. With the use of the Bio-Rad Protein Assay, the total concentration of protein in the BL21 cell lysate was determined to be 2.4 mg/mL for the Intimin−ECD-expressing strain and 2.2 mg/mL for JM109.

RESULTS AND DISCUSSIONS

A PSi 1D BPG microcavity contains a defect (symmetry breaking) layer sandwiched between two Bragg mirrors. The optical reflectance spectrum of a microcavity is characterized by narrow resonances that are very sensitive to the effective optical thickness of each layer. When the sensor is exposed to the target, the binding of target species inside the pores increases the effective refractive index of the pores and causes a red shift of the resonance. The total amount of red shift is linearly related to the amount of analyte captured by the sensor. Details of the sensor sensing principle, design, and optimization were described elsewhere.[21,22] Simulations show that for a microcavity with layers of 80% and 70% porosity, the sensor has a wavelength shift sensitivity of $\Delta\lambda/\Delta n$ ~500 nm/RI, where $\Delta\lambda$ is the shift of the resonance and Δn is the change of effective refractive index of the pores.[15,18] Assuming a detection system able of resolving a shift of 0.5 nm, the minimum Δn that can be detected is 1×10^{-3}, which is equivalent to an internal surface areal mass of ~50 pg/mm^2 for sensors with a 100 nm average pore diameter.[18]

A series of sensors derivatized with APTES and glutaraldehyde were exposed to Tir−IBD solutions with different concentrations from 0 to 1 mM. As shown in Figure 2, the red shift of the spectrum increases as the concentration of Tir−IBD increases. Since the red shift of the spectrum is approximately linearly related to amount of protein captured inside the microcavity, we conclude

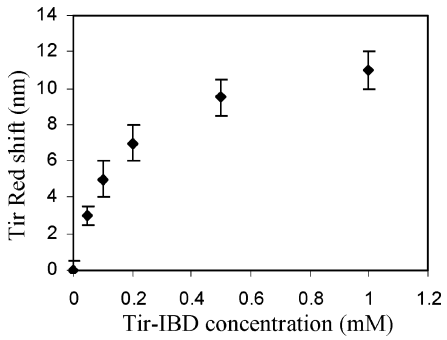

Figure 2. Red shift of the macroporous silicon microcavity reflectance dip as a function of the Tir−IBD concentration. The total volume of the solution applied to each sensor was 50 μL.

that the total amount of proteins immobilized in the sensor increases as the protein concentration increases. Thus, it is possible to prepare different surface concentrations of the probe molecule. At high Tir−IBD concentrations (~1 mM), the red shift saturates at ~12 nm, which is consistent with Langmuir adsorption isotherm behavior where all surface adsorption sites are filled and multilayer adsorption does not occur.

With the use of our model for the quantitative analysis of the sensor sensitivity, a 0.5 nm red shift of the microcavity corresponds to the capture of ~50 pg/mm^2 of protein inside the pores.[18] Thus, in this case, a 12 nm red shift corresponds to ~1.2 ng/mm^2 of Tir−IBD. Assuming that the total internal surface area of the sensor is 15 000 mm^2, the total mass of Tir−IBD needed to achieve a saturated surface coverage is ~18 μg or 1.8 nmol for the entire sensor with a 150 mm^2 top surface.

The kinetics of protein binding to surface-tethered receptors may be impacted by steric effects. These are exacerbated in the case of multivalent proteins.[23] Studies have shown that the performance of solid-phase sensors may depend on the probe molecule surface density.[24] To investigate the importance of this effect on the binding of Intimin−ECD, we studied the sensor response as a function of the Tir−IBD surface concentration and Intimin solution concentration. In this experiment, four identical sets of microcavity sensors were prepared. Each set contains six samples that were functionalized with different amounts of Tir−IBD as described above. Next, purified Intimin−ECD solutions with different concentrations (5−60 μM) were applied to each set of sensors. As shown in Figure 3, the optical red shift of the microcavities is related to the amount of both Tir−IBD and Intimin−ECD.

As expected, the amount of Intimin−ECD captured by the sensor depends on both the immobilized Tir−IBD concentration and the Intimin−ECD solution concentration. Figure 3 illustrates a general trend that for a fixed Tir−IBD receptor concentration the sensor red shift, hence the amount of Intimin−ECD captured, increases with the Intimin−ECD solution concentration. Also, for a fixed Intimin−ECD solution concentration, the sensor red shift increases with the Tir−IBD receptor concentration. In the latter case, the magnitude of the shift (amount of bound Intimin) tends to saturate at the highest Tir−IBD coverage. In our previous work, we had observed that the optimum surface coverage of biotin for

(21) Ouyang, H.; Fauchet, P. M. *Proc. SPIE-Int. Soc. Opt. Eng.* **2005**, *6005*, 6005081−60050815.
(22) Ouyang, H.; Lee, M.; Miller, B. L.; Fauchet, P. M. *Proc. SPIE-Int. Soc. Opt. Eng.* **2005**, *5926*, 59260J1−J11.
(23) Schuck, P. *Annu. Rev. Biophys. Biomol. Struct.* **1997**, *26*, 541−566.
(24) Jung, L. S.; Nelson, K. E.; Stayton, P. S.; Campbell, C. T. *Langmuir* **2000**, *16*, 9421−9432.

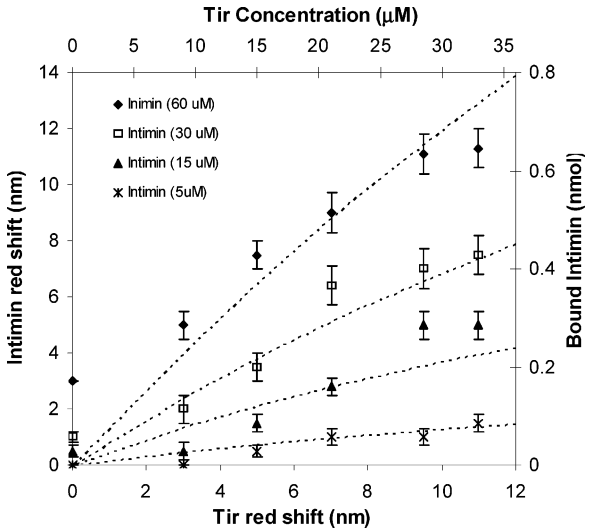

Figure 3. Red shift of sensors that were functionalized with different Tir−IBD concentrations after exposure to purified Intimin−ECD solutions with different concentrations from 5 to 60 μM. Theoretical calculation of the bound Intimin as a function of Tir concentration is plotted in the secondary axis using a K_d ~10^{-4} M. The agreement between the theoretical calculation and experimental data suggests a higher K_d for immobilized probes Tir−IBD.

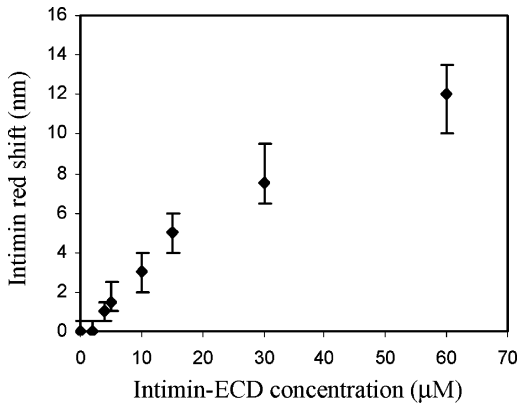

Figure 4. Dependence of the sensor red shift on the Intimin−ECD solution concentration. These sensors are functionalized with 1 mM Tir−IBD solutions.

binding streptavidin is ~50%.[12] A higher biotin surface coverage resulted in a lower streptavidin capture, which was attributed to steric effects associated with its "pocket-type" tight bonding (mechanical lock and key) structure.[24] For the Tir−IBD/Intimin−ECD system the binding pocket is "end-on" (binding sites are at the end of the cylindrical-like molecules),[25] and hence steric crowding at high Tir concentrations does not appear to impact binding. It can be seen from Figure 3 that when the Intimin−ECD concentration is higher than 30 μM some nonspecific binding of Intimin−ECD is detectable at zero Tir−IBD concentration. Hence, to achieve maximum Intimin−ECD detection sensitivity with minimum nonspecific binding, the sensors used in our quantitative analytical detection studies described below were functionalized with a saturated coverage of Tir−IBD by treating each sensor with 50 μL of 1 mM Tir−IBD.

We conducted simulations to investigate the effect of immobilization on the equilibrium dissociation constant K_d for Tir−IBD and Intimin−ECD using the following equation:

$$K_d = \frac{([\mathrm{Tir}_{total}] - [\mathrm{Int}_{bound}])([\mathrm{Int}_{total}] - [\mathrm{Int}_{bound}])}{[\mathrm{Int}_{bound}]}$$

where $[\mathrm{Int}_{total}]$ is the solution concentration of Intimin−ECD which varied from 0 to 60 μM, $[\mathrm{Int}_{bound}]$ is the amount of Intimin−ECD captured by the sensor, and $[\mathrm{Tir}_{total}]$ is the surface-immobilized concentration of Tir−IBD which we estimated from the red shift in Figure 2. It can be seen from the equation that for a given value of K_d, $[\mathrm{Int}_{bound}]$ can be plotted as a function of $[\mathrm{Tir}_{total}]$. In our simulation, the maximum Tir concentration was set at 36 μM (1.8 nmol/50 μL). The amount of Intimin captured by the sensor (= $([\mathrm{Int}_{bound}])(50\ \mu\mathrm{L})$) was calculated using different K_d values. The best fit solutions were obtained with K_d set to be 1×10^{-4} M. These simulation results are plotted on a secondary *x*- and *y*-axis as shown in Figure 3. Although this analysis provides a crude estimation of K_d, it nevertheless yields a value consistent with the expected much weaker association for immobilized probe receptors compared to that of free Tir−IBD and Intimin−ECD in solution. The increase of K_d by 2 orders of magnitude (from 0.3 $\times 10^{-6}$ to 1×10^{-4} M) may reflect steric factors that alter the binding pocket or a kinetic effect due to pH or concentration gradient within the porous structure.

An Intimin calibration curve using recombinant protein control solutions is shown in Figure 4. The sensor red shift is plotted as a function of the target concentration. The concentration sensitivity limit of the sensor is currently 4 μM of Intimin−ECD. Although the current concentration detection limit of the sensor is higher (less sensitive) than that of traditional proteomics techniques, such as silver staining in 2D-PAGE or ELISA, this label-free optical sensing method shows great potential due to its ease of fabrication and operation. This technology offers the potential to be developed for rapid, point-of-care diagnostic or laboratory sample screening applications where ultrasensitive detection (subpicomolar) sensitivity is not a concern. Using existing microelectronic techniques, one could easily shrink down the size scale of the sensor and integrate it into a microfluidic system to build a lab-on-a-chip device. This integration would reduce the total volume of sample required for the test. We estimate that our current detection limit corresponds to a mass sensitivity of ~600 ng/sensor by assuming that 10% of the protein in the 50 μL solution that was applied to the sensor was captured by the PSi matrix (~1 μL). The total internal surface area of the sensor is ~15 000 mm^2; thus, the areal mass sensitivity is ~50 pg/mm^2, which is consistent with the theoretical estimation.[18] Since the spot size of the measurement is approximately 1 mm^2, the amount of Intimin−ECD that contributed to the red shift is approximately 130 fmol.

To demonstrate selectivity, a 2 × 2 sensor array was designed. Two samples containing Tir−IBD and two samples without Tir−IBD were prepared. Sensors with and without Tir−IBD functionalization were exposed separately to cell lysate (supernatants) obtained from the BL21 *E. coli* cell line (expressing Intimin−ECD) and from the JM109 *E. coli* cell line (not expressing Intimin−ECD) prepared with a nearly equivalent total protein concentration (~2 mg/mL). A positive response should be obtained only when

(25) Luo, Y.; Frey, E. A.; Pfuetzner, R. A.; Creagh, A. L.; Knoechel, D. G.; Haynes, C. A.; Finlay, B. B.; Strynadka, N. C. *Nature* **2000**, *405*, 1073.

the sensor with Tir−IBD immobilized inside the pores is exposed to the protein mixture containing Intimin−ECD.

A 5 nm red shift was obtained from the Tir−IBD-functionalized sensor following exposure to the BL21 cell lysate containing Intimin−ECD. A very small shift (<1 nm) was detected from the Tir−IBD-functionalized sensor after exposure to the JM109 cell lysate solution that does not contain Intimin−ECD. The sensors prepared without Tir−IBD functionalization did not respond to the protein mixture with and without Intimin−ECD. The results indicate that the sensors can selectively detect Intimin−ECD from the protein mixture. From the red shift, we can estimate the Intimin−ECD concentration in the protein mixture with minimal background interference (nonspecific binding) using the calibration curve shown in Figure 4. A 5 nm red shift corresponds to a 15 μM concentration of Intimin−ECD. To validate the Intimin−ECD concentration in the cell lysate protein mixture, we used SDS−PAGE gel electrophoresis. Pure Intimin−ECD control solutions with known concentrations were run with the *E. coli* (BL21 and JM109) cell lysate solutions (both ∼2 mg/mL total protein), and the optical densities of the pure Intimin−ECD protein solution bands were compared. Using the gel analysis function in ImageJ (see the Supporting Information), we estimated the concentration of Intimin−ECD in the supernatant to be ∼14 μM, which is very close to the value predicted from the sensor optical response. No Intimin−ECD band was observed in the JM109 protein cell lysate, as expected.

To conclude, we have demonstrated the use of a macroporous silicon 1D PBG microcavity as a quantitative analytical device for optical label-free biosensing. The molecule binding events increase the effective refractive index of the sensor, which can be easily detected by monitoring the shift of the optical reflectance spectrum of the device. We have successfully functionalized the biosensors with Tir−IBD, a protein secreted by enteropathogenic *E. coli*. These protein sensors were able to selectively and quantitatively detect purified Intimin−ECD (target) binding to Tir−IBD (receptor). This work demonstrates for the first time the analytical capability of a macroporous 1D PBG sensor using a micromolar K_d protein bioconjugate system for which target specificity was validated in the testing of a complex bacterial cell lysate. In this sample, the target was a minority component (23%) of the total protein milieu. This is significant because our operating protocol utilized a long wash step (1−2 h) to minimize nonspecific binding. While this protocol compromises our lower limit of detection, the analytical capability is retained. Future studies will investigate methods to enhance the detection limit by exploring chemical nonspecific blocking agents and by upgrading our optical detection apparatus.

ACKNOWLEDGMENT

This work is supported by the National Science Foundation through Grant BES 0427919 and the National Institutes of Health (5K25AI060884-02).

SUPPORTING INFORMATION AVAILABLE

SDS−PAGE analysis results and calibration curve of the Intimin concentration. This material is available free of charge via the Internet at http://pubs.acs.org.

Received for review May 5, 2006. Accepted October 1, 2006.

AC0608366